Available online at www.easd.procedia.org
EASD Procedia EURODYN (2026) 97-105

EASD Procedia

EURODYN 2026
XIII International Conference on Structural Dynamics
M. Beer, C. Papadimitriou, H. Jensen, J. Chen, M. Broggi, J. Behrensdorf (eds.)
Hannover, Germany, 27.09.–01.10 2026

A CHARACTERIZATION METHOD FOR FATIGUE DAMAGE UNDER BROADBAND NON-STATIONARY NON-GAUSSIAN RANDOM VIBRATIONS

Wuyang Lei[1,2], Xiao Xiao[1,2], and Yu Jiang[1,2]

[1] College of Intelligent Science and Technology, National University of Defense Technology
Changsha 410073, China

[2] National Key Laboratory of Equipment State Sensing and Smart Support
Changsha 410073, China
e-mail:{leiwuyang,xiaoxiao25,jiangyu}@nudt.edu.cn

Keywords: Random vibration fatigue, Non-stationary and non-Gaussian, Rainflow counting, Broadband spectra.

Abstract. *Broadband non-stationary and non-Gaussian (NSNG) random vibrations widely exist in the service environments of complex mechanical systems. The rainflow counting method is considered the most accurate approach for evaluating fatigue damage under such conditions; however, it becomes computationally expensive when handling long-duration or high-frequency vibration data. To address this limitation, this study investigates the relationship between the statistical characteristics of broadband NSNG random signals and their fatigue damage obtained by rainflow counting. The results show that when the material fatigue exponent b is small, a positive correlation exists between the b-th order absolute moment of the vibration signal and its rainflow-counted fatigue damage. Based on this finding, a rapid fatigue evaluation method is proposed that bypasses rainflow counting by directly using the b-th order moment to characterize fatigue damage under broadband NSNG random vibrations. This approach provides a computationally efficient alternative for fatigue assessment in stochastic vibration environments.*

ISSN:2311-9020 © 2026 The Authors. Published by EASD Procedia.
Peer-review under responsibility of the Organizing Committee of EURODYN 2026.
doi: 10.47964/1326.10641.058

1 INTRODUCTION

Random vibration fatigue is a primary failure mechanism governing the structural integrity and reliability of complex mechanical, aerospace, and automotive systems. In real-world service environments, such as aerospace vehicles subjected to aerodynamic buffeting or ground vehicles experiencing rough road profiles, the dynamic loads frequently exhibit broadband, non-stationary, and non-Gaussian (NSNG) characteristics [1-3]. These NSNG processes are characterized by severe transient shocks, heavy-tailed probability distributions, and time-varying intensities, which significantly accelerate the accumulation of fatigue damage compared to stationary Gaussian vibrations.

Currently, the rainflow counting (RFC) method, combined with Miner's linear cumulative damage rule, remains the most accurate and universally accepted approach for evaluating fatigue damage in the time domain. However, the RFC algorithm involves highly nonlinear peak-valley extraction and cycle pairing processes. When applied to long-duration vibration data or large-scale finite element (FE) models with millions of degrees of freedom, the computational cost of time-domain RFC becomes prohibitively expensive, significantly hindering rapid design iterations and health monitoring.

To overcome this computational bottleneck, frequency-domain spectral methods have been widely adopted. Traditional spectral methods, such as the Dirlik and Tovo-Benasciutti models [4-6], estimate fatigue damage directly from the moments of the Power Spectral Density (PSD). While computationally efficient, these classical models are fundamentally predicated on the assumption of stationary Gaussian processes. When applied to NSNG vibrations, they fail to capture the heavy-tailed stress amplitude distributions caused by transient shocks, resulting in severe, sometimes catastrophic, underestimation of fatigue life [1, 3, 7-9].

To account for non-Gaussianity, numerous researchers have introduced the fourth-order statistical moment (kurtosis) as a correction factor to scale the Gaussian damage [10-12]. Although kurtosis-based corrections offer mathematical simplicity and computational convenience, they are still fundamentally developed under the assumption of stationarity. Consequently, when applied to highly non-stationary and severe non-Gaussian environments characterized by extreme kurtosis values, the prediction accuracy of these methods often deteriorates, highlighting the need for further improvement.

To address these limitations, this study investigates the intrinsic statistical drivers of fatigue damage under broadband NSNG random vibrations from a fundamental mathematical perspective. Rather than relying on fixed-order corrections, a novel characterization method based on the b-th order absolute moment of the vibration signal is proposed. The remainder of this paper is organized as follows: Section 2 introduces a high-fidelity NSNG signal generation method to ensure strict spectral control. Section 3 presents a new theoretical derivation linking the b-th moment to RFC damage. Section 4 provides extensive numerical validations across various broadband spectra. Finally, Section 5 draws the conclusions.

2 GENERATION OF NSNG RANDOM VIBRATION SIGNALS

To rigorously investigate the relationship between signal statistics and fatigue damage, it is imperative to generate NSNG signals that strictly preserve the target PSD while allowing independent control over the non-Gaussian characteristics. Conventional non-linear transformation methods often induce unacceptable spectral distortion. Therefore, an amplitude-phase modulation and spectrum recombination method is employed in this study.

Let $G_{xx}(f)$ be the target broadband PSD. The generation process can be summarized in the following steps:

(1) **Initial Modulation:** A stationary Gaussian signal $g(t)$ conforming to $Gxx(f)$ and a low-frequency modulation signal $m(t)$ are generated. To introduce non-Gaussianity, the modulation signal is transformed by an exponent p, yielding a preliminary modulated signal $y(t)=|m(t)|^p \cdot g(t)$.

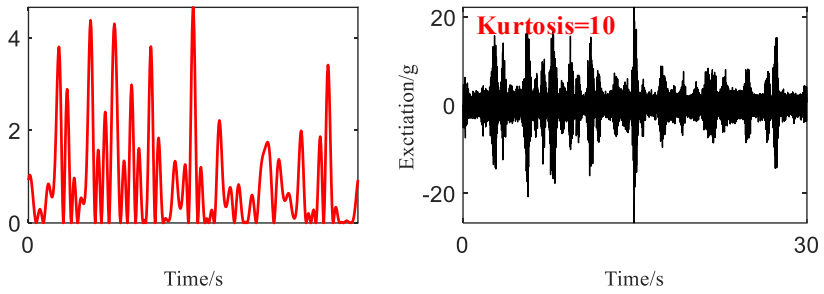
(2) **Phase Extraction:** The Fourier transform of $y(t)$ is computed to extract its phase spectrum $\phi_y(f) = \arctan\left[\mathrm{Im}(Y(f)) / \mathrm{Re}(Y(f))\right]$. The phase spectrum encodes the transient shock features and non-Gaussian characteristics of the modulated signal.

(3) **Spectrum Recombination:** The final NSNG signal $x(t)$ is synthesized by recombining the strictly defined target amplitude spectrum with the extracted phase spectrum $\phi_y(f)$ via the Inverse Fast Fourier Transform (IFFT):

$$x(t) = \mathcal{F}^{-1}\left\{\sqrt{G_{xx}(f)} \cdot e^{j\phi_y(f)}\right\}. \tag{1}$$

(4) **Iterative Kurtosis Control:** The kurtosis of the generated signal K_u is evaluated. If K_u is lower than the target kurtosis, the exponent p is incrementally increased to intensify the amplitude modulation; conversely, if K_u is too high, p is decreased.

A typical NSNG signal generated by this method, with a target kurtosis of 10, is illustrated in Fig. 1. As observed, the signal exhibits pronounced time-varying root-mean-square (RMS) characteristics, which is a distinct hallmark of non-stationary processes.



(a) modulation signal (b) non-stationary and non-Gaussian signal

Figure 1: Time-domain waveform of a typical synthesized non-stationary and non-Gaussian (NSNG) random vibration signal.

This iterative procedure rapidly converges, yielding an NSNG signal that simultaneously satisfies the exact target PSD (ensuring identical second-order statistics) and the target kurtosis, providing a pristine foundation for subsequent fatigue analysis.

3 DERIVATION OF THE B-TH MOMENT CHARACTERIZATION METHOD

According to the continuous formulation of Miner's rule, the expected fatigue damage intensity $\bar{D}$ (damage per unit time) for a stress process $x(t)$ can be defined through the rainflow cycle amplitude probability density function (PDF) $p_{\mathrm{RFC}}(S)$

$$\bar{D} = \frac{v_p}{C}\int_0^\infty S^b p_{RFC}(S)dS = \frac{v_p}{C} E_{RFC}\left[S^b\right]. \tag{2}$$

where v_p is the peak rate, C and b are material constants, and $E_{RFC}[\cdot]$ denotes the mathematical expectation over the rainflow measure.

For a broadband NSNG process, $p_{\mathrm{RFC}}(S)$ is highly complex and analytically intractable. However, the rainflow counting algorithm can be viewed mathematically as a nonlinear functional operator H that maps the instantaneous amplitude PDF of the signal $p_x(x)$ to the rainflow amplitude PDF $p_{\mathrm{RFC}}(S)$.

Based on the statistical energy dissipation equivalency in random processes, the higher-order statistical dispersion of the signal's instantaneous amplitudes inherently dictates the severity of the rainflow cycles. We introduce the *b*-th order absolute moment of the instantaneous signal, defined as:

$$M_b = E\left[|x(t)|^b \right] = \int_{-\infty}^{\infty} |x|^b \ p_x(x)dx . \tag{3}$$

For a fixed PSD geometry (i.e., the spectral shape remains constant), the frequency-domain distribution of energy is invariant. Consequently, the mapping operator H between the instantaneous probability measure and the rainflow probability measure behaves as an approximately linear scaling operator with respect to fractional statistical moments.

Therefore, it can be mathematically hypothesized that the *b*-th moment of the rainflow amplitudes $E_{RFC}\left[S^b \right]$ is directly proportional to the *b*-th absolute moment of the instantaneous signal $E\left[|x(t)|^b \right]$

$$E_{RFC}\left[S^b \right] = \Lambda(G_{xx}, b) \cdot E\left[|x(t)|^b \right]. \tag{4}$$

where $\Lambda(G_{xx}, b)$ is a generalized proportionality functional that depends strictly on the target PSD shape $G_{xx}(f)$ and the fatigue exponent *b*, but is remarkably insensitive to the phase variations that govern the non-Gaussianity (e.g., kurtosis).

Substituting Eq. (4) into Eq. (2), the fatigue damage intensity can be rewritten as:

$$\bar{D} = \left[\frac{v_p \cdot \Lambda(G_{xx}, b)}{C} \right] \cdot E\left[|x(t)|^b \right] \propto E\left[|x(t)|^b \right]. \tag{5}$$

Eq. (5) yields a profound conclusion: For any given broadband spectrum, the variation in fatigue damage caused by non-stationary and non-Gaussian temporal features exhibits a strong linear proportionality to the variation in the *b*-th order absolute moment of the signal. This implies that M_b can serve as a direct, standalone characterization parameter for NSNG fatigue damage, completely bypassing the complex reconstruction of $p_{\mathrm{RFC}}(S)$ and the computationally expensive time-domain rainflow counting process.

4 SIMULATION VALIDATION

To rigorously validate the proposed theoretical relationship, extensive numerical simulations were conducted utilizing massive NSNG datasets.

4.1 Simulation Setup

Two representative categories of broadband spectra were designed following the established criteria of literature [13]: the Spectral Width (SW) series and the Background Noise (BN) series. The overall root-mean-square (RMS) stress level for all signals was uniformly set to 10 MPa. To quantify the spectral broadness, the bandwidth parameter ε_v is introduced [14], which is calculated based on the spectral moments as:

$$\varepsilon_v = \sqrt{1 - \frac{m_2^2}{m_0 m_4}} \ , \ m_i = \int_0^{\infty} f^i G_{xx}(f)df \ . \tag{6}$$

where m_i is the *i*-th spectral moment. Generally, a process with $\varepsilon_v > 0.1$ is considered a broadband process.

(1) SW Series: Consists of 8 spectra (SW-1 to SW-8), where the bandwidth gradually expands from a narrow-band state to a pronounced broadband state, evaluating the

method's robustness against bandwidth variations. The specific spectral shapes and their corresponding bandwidth parameters ε_v are illustrated in Fig. 2.

(2) BN Series: Consists of 8 spectra (BN-1 to BN-8), wherein a wideband background noise of increasing intensity is superimposed onto a dominant resonance peak, simulating complex multi-source excitation environments. The detailed spectral configurations of the BN series are depicted in Fig. 3.

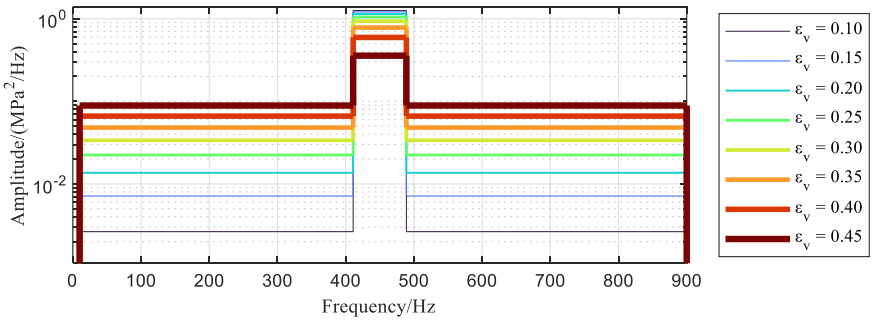


Figure 2: Power spectral density (PSD) models of the Spectral Width (SW) series.

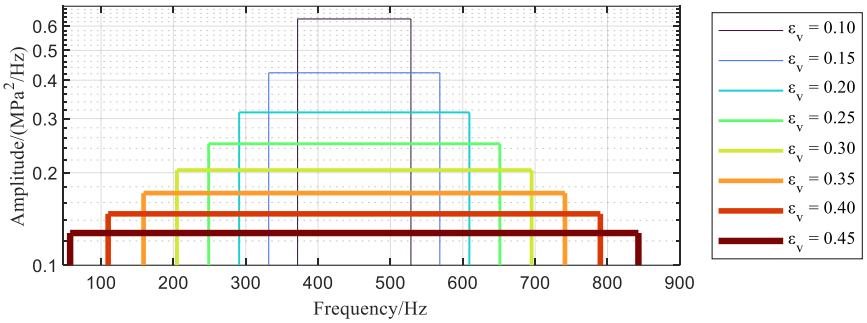


Figure 3: Power spectral density (PSD) models of the Background Noise (BN) series.

Using the generation method described in Section 2, 200 independent NSNG signal realizations were synthesized for each of the 16 PSDs. The kurtosis values of these signals were randomly and uniformly distributed in the severe non-Gaussian range of [5, 25]. The sampling frequency was set to 10 kHz, and the duration of each signal was 60 seconds.

For each of the 3,200 generated signals, the actual fatigue damage D_{RFC} was calculated using the time-domain RFC method for three typical fatigue exponents: $b \in [4,5,6]$. Simultaneously, the b-th order absolute moment M_b was computed directly from the time history.

4.2 Results and Discussion

To evaluate the proposed linear proportionality, scatter plots of the b-th order absolute moment versus the RFC fatigue damage were constructed. As a representative example, Fig. 4 presents the scatter plots for the SW series at a fatigue exponent of b=5. In each subplot, the 200 scatter points exhibit a close alignment with a linear trendline passing through the origin, indicating a linear correlation.

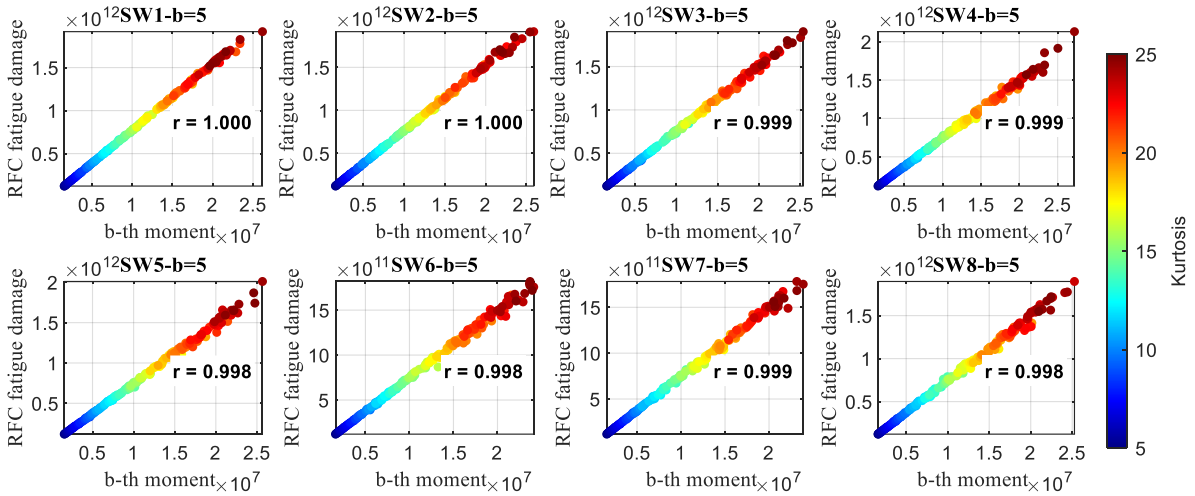


Figure 4: Scatter plots of the 5-th order absolute moment versus RFC fatigue damage for the Spectral Width (SW) series under fatigue exponent b=5

To provide a comprehensive statistical assessment without displaying redundant scatter plots, the Pearson correlation coefficients (r) were systematically calculated for all 16 tested spectra (SW and BN series) and for fatigue exponents $b \in \{4, 5, 6\}$. The results are summarized in Fig. 5. Analysis of Fig. 5 yields the following observations:

(1) High overall correlation. The Pearson correlation coefficients consistently exceed 0.99 across all tested bandwidths, background noise levels, and fatigue exponents. This indicates a strong linear relationship between the RFC fatigue damage (D_{RFC}) and the b-th order absolute moment (M_b).

(2) Influence of the fatigue exponent b. Within each subplot, a slight decrease in the correlation coefficient is observed as b increases from 4 to 6. This trend can be attributed to the fact that a larger b exponentially amplifies the contribution of extreme tail events (i.e., rare high-amplitude cycles) to the damage estimate. Consequently, the inherent statistical variability of such extreme events leads to a modest reduction in the deterministic linearity.

(3) Influence of spectral variations. As the spectrum broadens (from SW-1 to SW-8) and the background noise level increases (from BN-1 to BN-8), the correlation coefficients show a marginal decreasing trend. However, even under the most severe broadband noise condition combined with the highest tested fatigue sensitivity (BN-7 and BN-8 at b= 6), the correlation coefficient remains above 0.992.

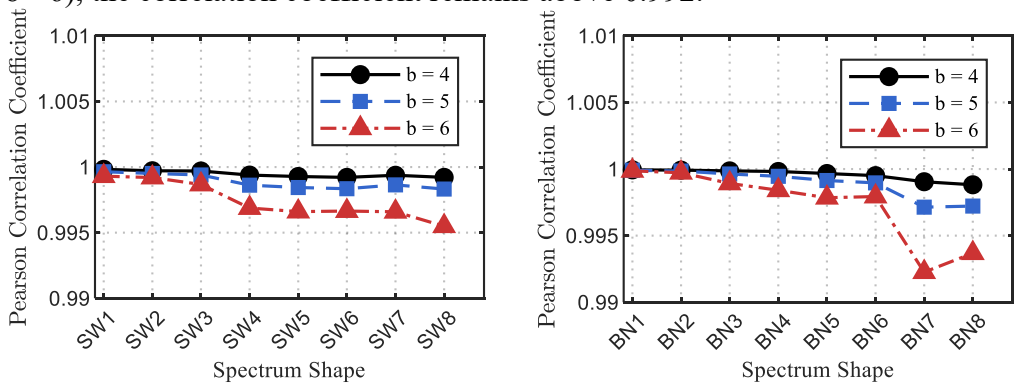


Figure 5: Variation of Pearson correlation coefficients (r) across different spectrum shapes and fatigue exponents: (left panel) Spectral Width (SW) series; (right panel) Background Noise (BN) series

To further quantify the stability of this proportionality, we define the damage-to-moment ratio:

$$\eta = D_{RFC} / M_b . \tag{7}$$

According to our theory, η should remain constant for a given PSD and b, regardless of the signal's kurtosis. Table 1 and Table 2 present the Coefficient of Variation (CV) of η for the SW and BN series, respectively. The CV reflects the relative fluctuation of the proportionality constant.

Spectral categories	Bandwidth parameter	b=4	b=5	b=6
SW-1	0.10	0.57	0.98	1.40
SW-2	0.15	0.70	1.21	1.81
SW-3	0.20	0.79	1.50	2.55
SW-4	0.25	1.05	2.03	3.38
SW-5	0.30	1.15	2.19	3.67
SW-6	0.35	1.21	2.32	3.95
SW-7	0.40	1.12	2.18	3.97
SW-8	0.45	1.26	2.48	4.46

Table 1 Coefficient of Variation (CV, %) of the damage-to-moment ratio for the Spectral Width (SW) series under different fatigue exponents.

Spectral categories	Bandwidth parameter	b=4	b=5	b=6
BN-1	0.10	0.36	0.57	0.81
BN-2	0.15	0.40	0.75	1.25
BN-3	0.20	0.51	1.05	1.91
BN-4	0.25	0.61	1.40	2.76
BN-5	0.30	0.77	1.58	2.79
BN-6	0.35	1.02	2.06	3.57
BN-7	0.40	1.35	2.84	4.84
BN-8	0.45	1.50	2.91	4.85

Table 2 Coefficient of Variation (CV, %) of the damage-to-moment ratio for the Background Noise (BN) series under different fatigue exponents.

A detailed observation of the data reveals that the CV exhibits an increasing trend with the enlargement of the bandwidth parameter ε_v and the fatigue exponent b, for instance, in the SW series (Table 1), the CV at b=6 increases from 1.40% for SW-1 to 4.46% for SW-8 as the spectrum broadens. A similar trend is observed in the BN series. This indicates that wider bandwidths and higher fatigue sensitivities introduce slightly more dispersion into the damage distribution.

Nevertheless, all reported CV values remain remarkably low (typically well below 5%). This minimal fluctuation demonstrates that the mapping coefficient Λ (from Eq. 4) is highly robust against extreme phase variations and severe kurtosis fluctuations (ranging from 5 to 25). The combined results of the high Pearson r and the low CV validate the theoretical derivation: when the fatigue exponent b is relatively small, the b-th order absolute moment can accurately characterize the fatigue damage potential of broadband NSNG vibrations.

5 CONCLUSION

This study proposed a rapid fatigue damage characterization method for broadband non-stationary and non-Gaussian (NSNG) random vibrations. Based on the theoretical mapping

between the rainflow probability measure and instantaneous statistical moments, it was analytically demonstrated that fatigue damage is intrinsically driven by the b-th order absolute moment of the signal.

Extensive numerical validations across 16 broadband spectra (covering bandwidth parameters ε_v from 0.10 to 0.45) and 3,200 NSNG signals with extreme kurtosis variations (5 to 25) yielded the following conclusions:

(1) There is an exceptionally strong positive linear correlation (Pearson $r > 0.99$) between the b-th order absolute moment of an NSNG signal and its rainflow-counted fatigue damage.

(2) The proportionality coefficient between damage and the b-th moment exhibits remarkable stability, with the Coefficient of Variation (CV) remaining strictly below 5% across all tested broadband conditions.

(3) For typical structural materials with relatively small fatigue exponents, the b-th order absolute moment can directly, accurately, and uniquely characterize fatigue damage. This method circumvents the computationally exhaustive rainflow counting algorithm, providing a highly efficient alternative for rapid fatigue assessment in complex stochastic environments.

REFERENCES

[1] A. Trapp, and P. Wolfsteiner, “Fatigue assessment of non-stationary random loading in the frequency domain by a quasi-stationary Gaussian approximation” In: International Journal of Fatigue 148 (2021), pp. 106214. DOI: 10.1016/j.ijfatigue.2021.106214.

[2] W. Lei, Y. Jiang, X. Zhou, H. Tang, and J. Zhang, “Vibration fatigue analysis of structures under non-stationary and non-Gaussian random excitation” In: Probabilistic Engineering Mechanics 79 (2025). DOI: 10.1016/j.probengmech.2025.103744.

[3] P. Wolfsteiner, and A. Trapp, “Modeling of statistical and spectral properties of non-Gaussian random vibration fatigue loads using Higher Order Spectra” In: International Journal of Fatigue 198 (2025), pp. 109004. DOI: 10.1016/j.ijfatigue.2025.109004.

[4] T. Dirlik, “Application of computers in fatigue analysis” University of Warwick, 1985.

[5] J.-B. Park, J. Choung, and K.-S. Kim, “A new fatigue prediction model for marine structures subject to wide band stress process” In: Ocean Engineering 76 (2014), pp. 144–151. DOI: 10.1016/j.oceaneng.2013.11.002.

[6] S.-H. Jun, and J.-B. Park, “Development of a novel fatigue damage model for Gaussian wide band stress responses using numerical approximation methods” In: International Journal of Naval Architecture and Ocean Engineering 12 (2020), pp. 755–767. DOI: 10.1016/j.ijnaoe.2020.09.005.

[7] A. Trapp, and P. Wolfsteiner, “Frequency-domain characterization of varying random vibration loading by a non-stationarity matrix” In: International Journal of Fatigue 146 (2021), pp. 106115. DOI: 10.1016/j.ijfatigue.2020.106115.

[8] W. Lei, Y. Jiang, Y. Tian, H. Tang, and J. Zhang, “Kurtosis transfer in MDOF systems under amplitude-modulated Non-Stationary Non-Gaussian Excitations: A Frequency-Domain decomposition approach” In: Mechanical Systems and Signal Processing 236 (2025), pp. 113059. DOI: 10.1016/j.ymssp.2025.113059.

[9] A. Trapp, and P. Wolfsteiner, “Fast assessment of non-Gaussian inputs in structural dynamics exploiting modal solutions” In: Mechanical Systems and Signal Processing 228 (2025), pp. 112396. DOI: 10.1016/j.ymssp.2025.112396.

[10] S. R. Winterstein, “Nonlinear vibration models for extremes and fatigue” In: Journal of Engineering Mechanics 114.10 (1988), pp. 1772–1790. DOI: 10.1061/(ASCE)0733-9399(1988)114:10(1772).

[11] C. Braccesi, F. Cianetti, G. Lori, and D. Pioli, “The frequency domain approach in virtual fatigue estimation of non-linear systems: The problem of non-Gaussian states of stress” In: International Journal of Fatigue 31.4 (2009), pp. 766–775. DOI: 10.1016/j.ijfatigue.2008.03.007.

[12] F. Cianetti, M. Palmieri, C. Braccesi, and G. Morettini, “Correction formula approach to evaluate fatigue damage induced by non-Gaussian stress state” In: Procedia Structural Integrity 8 (2018), pp. 390–398. DOI: 10.1016/j.prostr.2017.12.039.

[13] A. Zorman, J. Slavič, and M. Boltežar, “Vibration fatigue by spectral methods—A review with open-source support”. In: Mechanical Systems and Signal Processing 190 (2023), pp. 110149. DOI: 10.1016/j.ymssp.2023.110149

[14] E. H. Vanmarcke, “Properties of Spectral Moments with Applications to Random Vibration” In: Journal of the Engineering Mechanics Division 98.2 (1972), pp. 425–446. DOI: 10.1061/JMCEA3.0001593.